The Variation of Structure and Transporting Property in $SrRu_{1-x}Fe_xO_3$

Jung-Chul Park,[*] Don Kim,[†] Choong-Sub Lee,[‡] and Song-Ho Byeon[§]

Department of Nano Materials Science and Technology, Nano Applied Technology Research Center, Silla University, Busan 617-736, Korea
[†]*Department of Chemistry, Pukyong National University, Busan 608-737, Korea*
[‡]*Department of Physics, Pukyong National University, Busan 608-737, Korea*
[§]*College of Environment and Applied Chemistry, Institute of Natural Sciences, Kyung Hee University, Kyungki 449-701, Korea*
Received May 24, 2002

Key Words : Fe-substituted $SrRuO_3$, Bond-lengths and bond angles, Resistance

The ruthenium based perovskite oxide, $SrRuO_3$ has been intensively studied due to its diverse electronic and magnetic properties. The structure of $SrRuO_3$ is orthorhombic (a = 5.573 Å, b = 5.538 Å, c = 7.856 Å), which is similar to that of rare earth orthoferrite, $GdFeO_3$, but it can be considered as pseudo-cubic (a_p = 3.93 Å). However, the electrical property of both compounds is contradictory to each other, namely a good conductor for $SrRuO_3$ and an insulator for $GdFeO_3$. This might be due to the different electron configurations as $GdFeO_3$ adopts the high spin $t_{2g}^3e_g^2$ of $Fe^{3+}$and $SrRuO_3$ the low spin $t_{2g}^4e_g^0$ of Ru^{4+}.

Recently, the electronic structural variation of $ARuO_3$ (A = Ca, Sr, and Ba) has been discussed using X-ray photoelectron spectroscopy, ultraviolet photoelectron spectroscopy, and Rietveld fitting of the XRD data.[1] The ionic radii of A cations (Ca=1.34 Å, Sr=1.44 Å, and Ba=1.61 Å) induces the distorted orthorhombic, particularly hexagonal symmetry for Ba compound. Moreover, the variation in Ru-O and Ru-Ru bond distances has a great influence on the electrical and magnetic properties of these compounds.

Some reports on the partial substitution of metal cations in Ru sites of $ARuO_3$. (A=Sr, Ca) have been issued. $SrTi_{1-x}Ru_xO_{3-\delta}$ ($0 \le x \le 1$) deposited films are cubic or pseudo-cubic over the whole composition range with the lattice parameters increasing continuously with the concentration of Ru^{4+}, which correspondingly results in the conductivity variation from insulating to metallic behavior.[2] The magnetic and transport properties of $CaMn_{1-x}Ru_xO_3$ ($0 < x \le 0.8$) were studied by Maignan *et al.* using resistivity and ac-susceptibility measurements, and they explained that the inducement of ferromagnetism and metallicity in the antiferromagnetic $CaMnO_3$ matrix is due to the valence combination (Ru^{5+} creating Mn^{3+}), which allows double exchange through the hybridization between Ru and Mn e_g orbitals.[3]

As previously reported, $SrFeO_{3-x}$ ($0 \le x \le 0.5$) is particularly interesting because of not only the unusual oxidation state of Fe^{4+} but also the wide range of oxygen non-stoichiometry. Takano *et al*. reported that the $SrFeO_{3-x}$ phases (x = 2.50, 2.73, 2.86, and 3.00) exist in different structures.[4] The perovskite cell is cubic for $2.88 \le x \le 3.00$ and tetragonal (or orthorhombic) for $2.72 \le x \le 2.88$. It should be pointed out that the $SrFeO_{2.5}$ phase with brownmillerite structure is shown to derive from the cubic $SrFeO_3$ unit cell by periodic removal of O atoms *via* [101] directions. Therefore, the solid-solution between $SrRuO_3$ and $SrFeO_{3-x}$ is of great interest as the ionic radius of the cations are quite similar (0.620 Å for Ru^{4+}, 0.645 Å for Fe^{3+}, and 0.585 Å for Fe^{4+})[5] and the different electronic configuration may have a great effect on the transporting properties of $SrRu_{1-x}Fe_xO_3$. In the present paper, we explore the electronic and crystal structure of $SrRu_{1-x}Fe_xO_3$ ($0 \le x \le 0.5$) in order to explain the variation of transporting properties of Fe-substituted $SrRuO_3$.

Experimental Section

The compounds in the $SrRu_{1-x}Fe_xO_3$ ($0 \le x \le 0.5$) solid solution were prepared by typical solid state reactions. Well ground stoichiometric mixtures of $SrCO_3$, RuO_2, and Fe_2O_3 were heated at 900 °C for 12 h in air. The ground residues were pelletized and heated at 1150 °C for 24 h in air. The final treatment was performed on pellets at 1200 °C for 24 h in air.

The formation of a single phase was confirmed by powder X-ray diffraction (XRD). The patterns for structure refinement were recorded on a rotating anode installed diffractometer with an X-ray source of 40 kV, 300 mA. The Cu Kα radiation used was monochromated by a curved-crystal graphite. The data were collected with a step-scan procedure in the range 2θ = 20-100° with a step width of 0.02° and a step time of 1 s. The refinements of reflection positions and intensities were carried out using the Rietveld analysis program RIETAN (Izumi *et al*., 1987). Mössbauer spectroscopic studies were carried out at 300 K with Co^{57} source doped in metallic rhodium which was oscillated in a sinusoidal mode. The Doppler velocity of spectra was calibrated with α-Fe foil (25 μm in thickness). The electrical resistance of polycrystalline pellets was measured using a standard four probe method.

Results and Discussion

XRD diffraction patterns of $SrRu_{1-x}Fe_xO_3$ ($0 \le x \le 0.5$) are shown in Figures 1-2. The refined structural parameters obtained from the Rietveld fitting of the XRD data are given

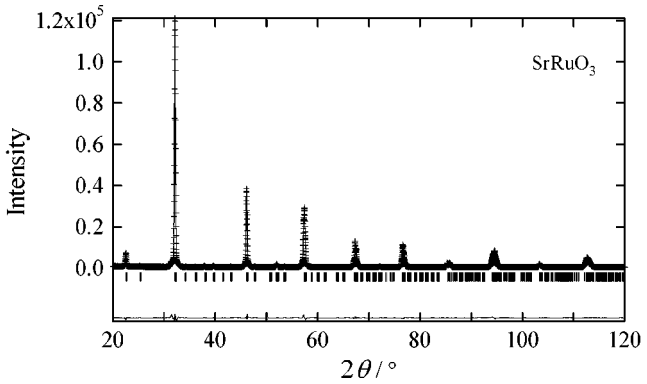

Figure 1. The experimental (top), fitted (middle), and difference (bottom) of X-ray diffraction pattern of $SrRuO_3$.

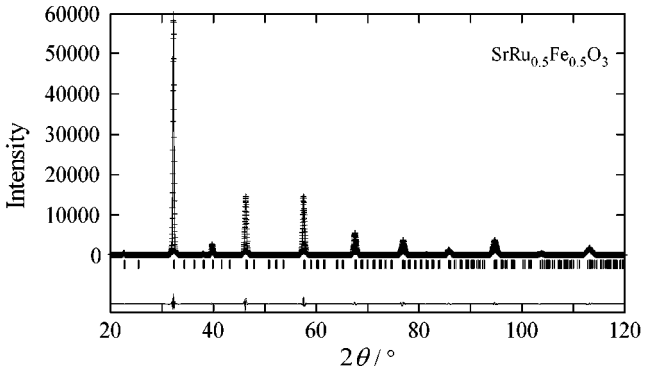

Figure 2. The experimental (top), fitted (middle), and difference (bottom) of X-ray diffraction pattern of $SrRu_{0.5}Fe_{0.5}O_3$.

Table 1. The structural parameters obtained from the Rietveld fitting of the XRD data

Compounds	Reliability factors (%)				Lattice parameters (Å)		
	R_I	R_{WP}	R_P	R_E	*a*	*b*	*c*
$SrRuO_3$	1.78	8.84	5.4	2.89	5.5704(1)	7.8499(2)	5.5356(1)
$SrRu_{0.9}Fe_{0.1}O_3$	1.68	8.43	5.41	3.72	5.5699(1)	7.8471(2)	5.5359(1)
$SrRu_{0.8}Fe_{0.2}O_3$	1.09	8.08	5.23	3.89	5.5686(1)	7.8397(2)	5.5374(1)
$SrRu_{0.7}Fe_{0.3}O_3$	1.13	6.66	4.64	3.99	5.5657(1)	7.8323(2)	5.5375(1)
$SrRu_{0.6}Fe_{0.4}O_3$	1.15	7.01	4.99	4.17	5.5604(2)	7.8307(3)	5.5426(2)
$SrRu_{0.5}Fe_{0.5}O_3$	0.81	8.94	6.7	4.32	5.5475(9)	7.8235(4)	5.5490(9)

in Table 1, and the bond lengths and bond angles are listed in Table 2. The XRD data indicate that $SrRu_{1-x}Fe_xO_3$ are orthorhombically distorted $GdFeO_3$ type structure with space group Pnma. Particularly, the lattice parameters, *a* and *b* gradually increase with increasing Fe-substitution, whereas the lattice parameter, *c* decreases, as shown in Table 1. In order to determine the valence state of Fe, Mössbauer spectroscopy was used. As shown in Figure 3, the valence state of iron in $SrRu_{1-x}Fe_xO_3$ (x = 0.1, 0.2, 0.3, 0.4, and 0.5) is determined to be Fe(III) with the isomer shifts, δ = 0.24, 0.26, 0.27, 0.28, and 0.30 mm/s, respectively.[6-8] As above mentioned, the magnetic and transport properties of the $CaMn_{1-x}Ru_xO_3$ ($0 < x \leq 0.8$) were studied by Maignan *et al.*,[3] and they explained that the inducement of ferromagnetism

Table 2. The bond lengths and bond angles obtained from the Rietveld data

Compounds	Bond length (Å)		Bond angle (deg)	
$SrRuO_3$	Ru-O1 (×2)	1.968(2)	Ru-O1-Ru	171.6(9)
	Ru-O2 (×2)	1.991(9)	Ru-O2-Ru	160.3(4)
	Ru-O2 (×2)	1.994(9)		
$SrRu_{0.9}Fe_{0.1}O_3$	RuFe-O1 (×2)	1.964(2)	RuFe-O1-RuFe	172.1(9)
	RuFe-O2 (×2)	1.972(9)	RuFe-O2-RuFe	162.4(4)
	RuFe-O2 (×2)	2.001(9)		
$SrRu_{0.8}Fe_{0.2}O_3$	RuFe-O1 (×2)	1.967(2)	RuFe-O1-RuFe	170.5(9)
	RuFe-O2 (×2)	1.95(1)	RuFe-O2-RuFe	166.1(4)
	RuFe-O2 (×2)	2.010(9)		
$SrRu_{0.7}Fe_{0.3}O_3$	RuFe-O1 (×2)	1.967(2)	RuFe-O1-RuFe	169.0(9)
	RuFe-O2 (×2)	1.95(1)	RuFe-O2-RuFe	168.2(3)
	RuFe-O2 (×2)	2.00(1)		
$SrRu_{0.6}Fe_{0.4}O_3$	RuFe-O1 (×2)	1.978(2)	RuFe-O1-RuFe	163.7(8)
	RuFe-O2 (×2)	1.96(2)	RuFe-O2-RuFe	169.8(5)
	RuFe-O2 (×2)	1.98(2)		
$SrRu_{0.5}Fe_{0.5}O_3$	RuFe-O1 (×2)	2.001(2)	RuFe-O1-RuFe	155.7(6)
	RuFe-O2 (×2)	1.92(1)	RuFe-O2-RuFe	176.2(6)
	RuFe-O2 (×2)	2.01(1)		

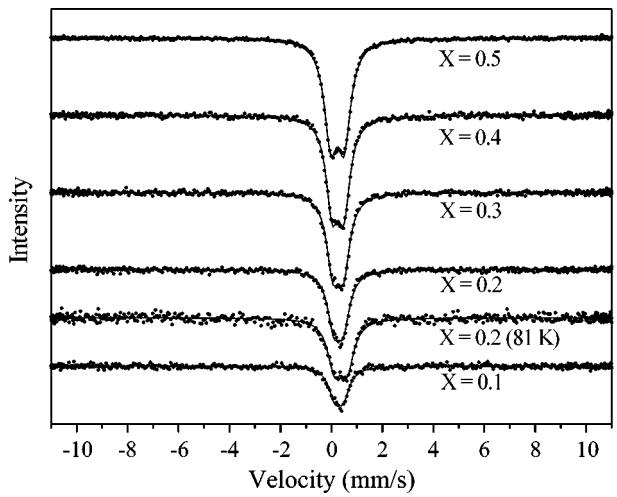

Figure 3. Mössbauer spectra of $SrRu_{1-x}Fe_xO_3$ collected at room temperature and 81 K.

and metallicity in the anti-ferromagnetic $CaMnO_3$ matrix is due to the valence combination (Ru^{5+} creating Mn^{3+}), which allows double exchange through the hybridization between Ru and Mn e_g orbital. In our system, as Fe^{3+} species are introduced into the $SrRuO_3$ lattice according to the formula of $SrRu^{4+}_{1-2x}Ru^{5+}_xFe^{3+}_xO_3$, Ru^{5+} species are formed. So, the local symmetry of $(Ru,Fe)O_6$ octahedra including (Ru,Fe)-O bond lengths and (Ru,Fe)-O-(Ru,Fe) bond angles may be considerably different from that of RuO_6 ones. The $SrRuO_3$ compound has a structure derived from the cubic perovskite structure. In this structure, the tolerance factor, $t = (R_{Sr^{2+}} + R_{O^{2-}})/\sqrt{2}\,(R_{Ru^{4+}} + R_{O^{2-}})$ which relates the Sr-O and Ru-O bond lengths, represents ideal bond-length matching for t = 1. A $t \approx 1$ at high temperature results in a $t < 1$ at lower temperature. A $t < 1$ place the Ru-O bonds under com-

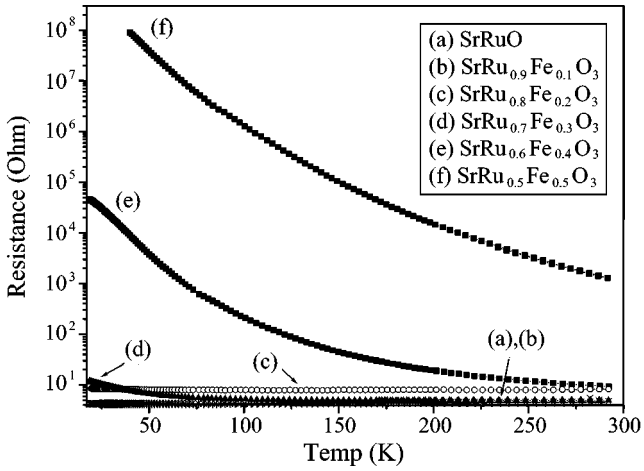

Figure 4. The electrical resistance of $SrRu_{1-x}Fe_xO_3$ as a function of temperature.

pression and Sr-O bonds under tension. This incompatibility can be relieved by a cooperative rotation of the RuO_6 octahedra that bends the Ru-O-Ru bond. As listed in Table 2, the $SrRu_{1-x}Fe_xO_3$ compounds has different bond lengths, in particular (Ru,Fe)-O_1(× 2) = 2.00 Å, (Ru,Fe)-O_2 (× 2) = 1.92 Å, and (Ru,Fe)-O_2 (× 2) = 2.01 Å for $SrRu_{0.5}Fe_{0.5}O_3$ compound, which discloses that the Fe^{3+} species create Ru^{5+} species as the longer (2.01 Å) and the shorter bond-length (1.92 Å) exist in (Ru,Fe)-O_2 sheets compared with those of $SrRuO_3$. It should be pointed out that the (Ru,Fe)-O_2 bond lengths manifest the strength of hybridization between Ru 4d and O 2p states, which is correlated with the transport properties of these compounds. Moreover, the (Ru,Fe)-O_1-(Ru,Fe) bond angles are continuously decreased with increasing the contents of Fe, whereas (Ru,Fe)-O_2-(Ru,Fe) bond angles are gradually increased toward 180°. It is well known that in La_2CuO_4-related superconductors the Cu-O-Cu bond angle would straighten out to 180°, which would remove the mixed symmetry.[9,10] Such a straightening results in an orthorhombic- to -tetragonal transition, and superconductivity vanishes in the tetragonal phase. As listed in Table 1, c/a values continuously decrease with increasing Fe-substitution, *i.e.* 1.0063 for $SrRuO_3$ and 0.9997 for $SrRu_{0.5}Fe_{0.5}O_3$, which shows the appearance of tetragonal character in $SrRu_{1-x}Fe_xO_3$ series. These interpretations are well coincident with the resistance results of $SrRu_{1-x}Fe_xO_3$ series as shown in Figure 4.

Conclusion

The $SrRu_{1-x}Fe_xO_3$ ($0 \le x \le 0.5$) solid solutions were prepared by typical solid state reactions. The XRD data indicate that $SrRu_{1-x}Fe_xO_3$ are orthorhombically distorted $GdFeO_3$ type structure with a space group Pnma. Particularly, the lattice parameters *a* and *b* gradually decrease with increasing Fe-substitution, whereas the lattice parameter, *c* increases. The *c*/*a* values continuously decrease with increasing Fe-substitution, *i.e.* 1.0063 for $SrRuO_3$ and 0.9997 for $SrRu_{0.5}$-$Fe_{0.5}O_3$, which shows the appearance of tetragonal character in $SrRu_{1-x}Fe_xO_3$ series. By using Mössbauer spectroscopy, the valence state of iron in $SrRu_{1-x}Fe_xO_3$ (x = 0.1, 0.2, 0.3, 0.4, and 0.5) is determined to Fe(III). The Fe-substituted $SrRuO_3$ has different bond lengths, in particular (Ru,Fe)-O_1 (× 2) = 2.00 Å, (Ru,Fe)-O_2 (× 2) = 1.92 Å, and (Ru,Fe)-O_2 (× 2) = 2.01 Å for $SrRu_{0.5}Fe_{0.5}O_3$ compound, which notifies us that the Fe^{3+} species create Ru^{5+} species as the longer (2.01 Å) and the shorter bond-length (1.92 Å) exist in (Ru,Fe)-O_2 sheets compared with those of $SrRuO_3$. The (Ru,Fe)-O_1-(Ru,Fe) bond angles are continuously decreased with increasing the contents of Fe-substitution, whereas (Ru,Fe)-O_2-(Ru,Fe) bond angles are gradually increased toward 180°. These structural behaviors are well coincident with the resistance results of $SrRu_{1-x}Fe_xO_3$ series.

Acknowledgment. This work was supported by Korean Research Foundation Grant (KRF-2000-015-DP0298).

References

1. Rama Rao, M. V.; Sathe, V. G.; Sornadurai, D.; Panigrahi, B.; Shripathi, T. *Journal of Physics and Chemistry of Solids* **2001**, *62*, 797.
2. Gupta, A.; Hussey, B. W.; Shaw, T. M. *Materials Research Bulletin* **1996**, *31*, 1463.
3. Maignan, A.; Martin, C.; Hervieu, M.; Raveau, B. *Solid State Communication* **2001**, *117*, 377.
4. Takano, M.; Nakayama, N.; Bando, Y.; Takeda, Y.; Kanno, K.; Takada, T.; Yamamota, O. *J. Sol. State Chem.* **1986**, *63*, 237.
5. Shannon, R. D. *Acta Cryst.* **1976**, *32*, 751.
6. Demazeau, G.; Fabritchnyi, P.; Fournes, L.; Darracq, S.; Presniakov, I. A.; Pokholok, K. V. *J. Mater. Chem.* **1995**, *5*, 553.
7. Nasu, S. *Hyperfine Interactions* **1994**, *90*, 59.
8. Cao, X.; Koltypin, Yu.; Katabi, G.; Prozorov, R.; Felner, I.; Gedanken, A. *J. Mater. Chem.* **1997**, *7*, 1007.
9. Goodenough, J. B.; Manthiram, A.; Zhou, J. *Mat. Res. Soc. Symp. Proc.* **1989**, *156*, 339.
10. Goodenough, J. B. *MRS Bulletin* 1**990**, May, 23.